Investigation of the Core Radial Electric Field in Wendelstein 7-X Plasmas

N.A. Pablant[1], A. Dinklage[2], M. Landreman[4], A. Langenberg[2], A. Alonso[5], C.D. Beidler[2], M. Beurskens[2], M. Bitter[1], S. Bozhenkov[2], R. Burhenn[2], L.F. Delgado-Aparicio[1], G. Fuchert[2], D.A. Gates[1], J. Geiger[2], K.W. Hill[1], U. Hoefel[2], M. Hirsch[2], J. Knauer[2], A. Krämer-Flecken[6], S. Lazerson[1], H. Maassberg[2], O. Marchuk[6], N.B. Marushchenko[2], D.R. Mikkelsen[1], E. Pasch[2], S. Satake[3], H. Smith[2], J. Svensson[2], P. Traverso[7], Y. Turkin[2], P. Valson[2], J.L. Velasco[5], G. Weir[2], T. Windisch[2], R.C. Wolf[1], M. Yokoyama[3], D. Zhang[2] and the W7-X Team

[1]*Princeton Plasma Physics Laboratory, Princeton, NJ, USA*

[2]*Max-Planck-Institut für Plasmaphysik,Greifswald, Germany*

[3]*National Institute for Fusion Science, Toki, Japan*

[4]*University of Maryland, College Park, MD, USA*

[5]*Laboratorio Nacional de Fusión – CIEMAT, Madrid, Spain*

[6]*Forschungszentrum Jülich , Jülich, Germany*

[7]*Auburn University, Auburn, AL, USA*

I. Introduction

Perpendicular plasma flow profiles from the first operational phase of the Wendelstein 7-X stellarator (W7-X) have been measured through the use of x-ray spectroscopy. These perpendicular plasma flow profiles are closely related to the radial electric field (E_r) through the force balance equation. In stellarator plasmas the neoclassical particle fluxes are not intrinsically ambipolar, which leads to the formation of a radial electric field that enforces ambipolarity. The details of the Er profile are expected to have a strong effect on both the particle and heat fluxes as well as the bootstrap current [1]. Initial measurements of the perpendicular plasma flow ($u_\perp$) and the inferred Er profiles in W7-X are presented and compared with predictions from neoclassical theory.

II. Diagnostic Method

Measurements of the plasma flow are made using the x-ray imaging crystal spectrometer (XICS). The XICS diagnostic relies on spectral emission from highly charged argon ions introduced into the plasma. The raw measurements from the XICS system provide a one dimensional wavelength resolved image of line integrated emission. The line integrated flow velocity profiles are found from the Doppler shift of the spectral lines. Tomographic inversion, using a known plasma equilibrium is used to infer the local plasma parameters from the line integrated data [2, 3]. A description of the XICS system on W7-X can be found in Ref. 4 and the diagnostic concept has been explained in detail by Bitter *et al.* in Ref. 5.

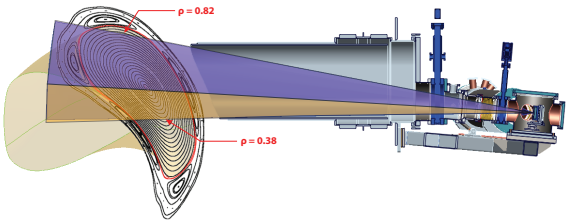

Figure 1: *Viewing geometry of the the XICS diagnostic on W7-X.*

The XICS viewing geometry, as seen in Fig.1, is primarily sensitive to the component of the velocity that is perpendicular to the magnetic field lines. The flow velocity in a stellarator is not expected to be constant on a flux surface, and this variation must be accounted for as part of the tomographic inversion. A simple form for the variation of the perpendicular flow on a flux surface can be found using the the radial force balance equation given the assumption that the plasma potential and plasma pressure are flux surface functions. With these assumptions the local perpendicular flow, $u_\perp$, can be related to the flux surface average flow, $U_\perp$, by the following expression:

$$u_\perp = fU_\perp, \quad f = -\frac{\langle B \rangle}{\langle |\nabla \rho| \rangle} \left(\frac{B \times \nabla \rho}{B^2} \right) \tag{1}$$

Where $\rho = \sqrt{\psi/\psi_{edge}}$ and $\langle \cdot \rangle$ denotes a flux surface average. Additional details on the derivation of this expression are given in Ref. 6. In the current work parallel velocity is neglected.

To derive the radial electric field from the flux surface averaged perpendicular flow velocity the radial force balance equation can be used.

$$\langle E_r \rangle = \frac{1}{en_I Z_I} \frac{\partial p_I}{\partial \rho} \langle |\nabla \rho| \rangle - \langle u_\perp B \rangle \tag{2}$$

Where p_I, n_I and Z_I denote the pressure, density and charge of the ion species being measured. The pressure gradient term is small for measurements of argon with the flat pressure profiles seen at W7-X, and has been neglected in the results shown in this work.

The achievable spatial and temporal resolution of the XICS measurements is limited by the intensity of the argon emission, and is therefore dependent on the amount of injected argon and the plasma conditions. For typical W7-X discharges with argon injection, flow velocity measurements can be made with temporal and spatial resolutions of 10ms and 2cm respectively and an accuracy of $\approx$1 km/s, which corresponds to a line shift of 0.01 $m\mathring{A}$ (0.025 $pixels$), and ultimately to accuracy in Er of $\approx$2.5 kV/m. The accuracy of the velocity measurements can be improved substantially by increasing the integration time through binning of multiple frames.

II. Core Electron Root Confinement (CERC)

During the first W7-X campaign hydrogen and helium plasmas were produced using up to 4 MW of centrally deposited electron cyclotron radiofrequency heating (ECRH). Typical plasmas had central electron tempertures of 6-8 keV, central ion temperatures of 1.5-2.1 keV and central densities in the range of 2-6$\times 10^{19}$ m^{-3} [7]. In previous stellarator experiments this set

of conditions, with centrally peaked electron temperature profiles and $T_e \gg T_i$, is associated with the development of a positive radial electric field in the plasma core [8].

Radial electric field profiles inferred from the XICS diagnostic confirm the expected existence of a postive radial electric field for plasmas produced during the first W7-X experimental campaign (see Fig.2). The general shape and magnitude of the E_r profiles has also been confirmed through plasma flow measurements made available through the correlation reflectometry diagnostic [9].

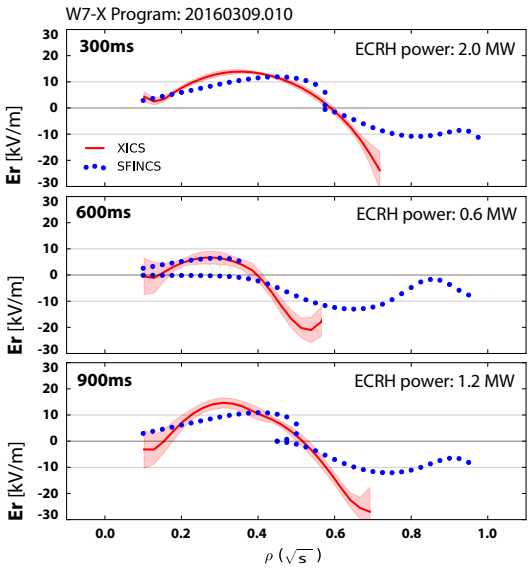

Figure 2: *Radial electric field profiles (E_r) infered from XICS velocity measurements. Spatial resolution is limited in the XICS measurements by strong smoothing during the inversion process. Also overlayed are calculated E_r profiles from the* SFINCS *neoclassical code.*

A plasma program was developed for the W7-X OP1.1 campaign to examine the effect of the input power on the radial electric field [10]. The program consists of three distinct steps of injected ECRH power (2.0 MW, 0.6 MW and 1.3 MW) in a plasma with a fixed density profile. The time history of this discharge can be seen in Fig.3. Additional details on these CERC discharges, including detailed plasma profiles can be found in [10].

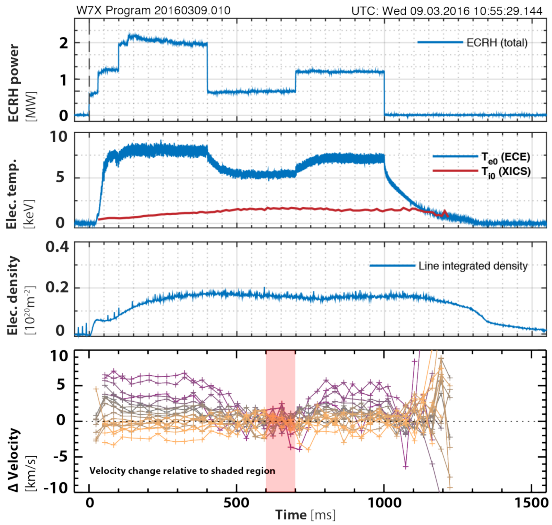

Figure 3: *Time traces for W7-X CERC discharge. For clarity, the change in velocity seen in individual XICS sightlines is shown relative to the value at 650 ms. Purple and yellow lines represent views above and below the magnetic axis respectively (see Fig.1).*

The E_r profiles in Fig.2 show that both the low and high power phases of the program have an electron-root solution in the core of the plasma. However, the magnitude and radial extent of the core positive E_r changes between the high and low power phases; the postive E_r region shrinks by about 30% when the power is reduced, with a corresponding decrease in magnitude.

The evolution of E_r can be seen by looking at the change over time of the line integrated velocity measurements. In Fig.3 the line integrated velocity of each XICS sightline is shown relative to its value in the low power phase. As soon as the injected power is stepped up or down, both the flow velocity and the electron temperature begin

to change. The time for equilibration, both for the flow velocity and the electron temperature is approximately 100 *ms*. Within the time resolution of the XICS measurements used for this analysis, 30 *ms*, the electron temperature and velocity appear to change simultaneously, which is consistent with the neoclassical understanding of E_r.

The profiles and dynamic behavior of the radial electric field seen during this experiment are similar to what has been seen previously in CERC plasmas on many stellarator devices such as LHD [2], W7-AS [11], TJ-II [12] and HSX [13] (see Ref. 8).

III. Comparsion to neoclassical calculations

Several neoclassical codes are available that can calculate radial electric field based on measured plasma profiles through the enforcement of ambipolarity of the particle fluxes. Three of these codes, SFINCS [14], DKES [15] and NTSS [16], have been run for the program shown in Fig.3. Each of these codes take slightly different approaches in solving to the drift kinetic equations, and find nearly identical solutions for the ambipolar E_r profiles. The neoclassical calculations are based on the measured electron temperature (T_e) and density (n_e) profiles from Thomson scattering[17], ion temperature (T_i) profiles from XICS, and an assumption of a pure hydrogen plasma with $Z_{eff} = 1$ (see Ref. 10).

A comparison of the E_r profiles from XICS and SFINCS is shown in Fig.2. Good agreement is seen, both in the magnitude and general shape of the E_r profile and in the radial location of the crossover from electron-root to ion-root. Predictions from the DKES are very similar, and are in general agreement with both the XICS and SFINCS profiles. The general agreement between the measured and predicted E_r profiles provides confidence in the validity of the neoclassical predictions in W7-X and their applicability for both experimental calculation of neoclassical quantities and their use in prediction for future machine performance.

Research supported by the U.S. DOE under Contract No. DE-AC02-09CH11466 with Princeton University. This work has been carried out within the framework of the EUROfusion Consortium and has received funding from the Euratom research and training programme 2014-2018 under grant agreement No 633053. The views and opinions expressed herein do not necessarily reflect those of the European Commission.

References

[1] Maaßberg, H. et al. Physics of Plasmas, **16**, 7, 072504 (2009).
[2] Pablant, N.A. et al. Plasma Physics and Controlled Fusion, **58**, 4, 045004 (2016).
[3] Pablant, N.A. et al. Review of Scientific Instruments, **85**, 11, 11E424 (2014).
[4] Pablant, N. et al. Europhysics Conference Abstracts, **38F**, P1.076 (2014).
[5] Bitter, M. et al. Review of Scientific Instruments, **81**, 10, 10E328 (2010).
[6] Arévalo, J. et al. Nuclear Fusion, **53**, 2, 023003 (2013).
[7] König, R. et al. 43rd EPS Conference on Plasma Physics, I2.108 (2016).
[8] Yokoyama, M. et al. Nuclear Fusion, **47**, 9, 1213 (2007).
[9] Hirsch, M. et al. Proceedings of Science, **ECPD2015**, 111 (2015).
[10] Dinklage, A. et al. 43rd EPS Conference on Plasma Physics, O2.107 (2016).
[11] Romé, M. et al. Plasma Physics and Controlled Fusion, **48**, 3, 353 (2006).
[12] Castejón, F. et al. Nuclear Fusion, **42**, 3, 271 (2002).
[13] Briesemeister, A. et al. Plasma Physics and Controlled Fusion, **55**, 1, 014002 (2013).
[14] Landreman, M. et al. Physics of Plasmas, **21**, 4, 042503 (2014).
[15] van Rij, W.I. and Hirshman, S.P. Physics of Fluids B, **1**, 3, 563 (1989).
[16] Turkin, Y. et al. Physics of Plasmas, **18**, 2, 022505 (2011).
[17] Pasch, E. et al. 43rd EPS Conference on Plasma Physics, P4.016 (2016).